Statistics and Probability Letters 144 (2019) 9–15

Contents lists available at ScienceDirect

Statistics and Probability Letters

journal homepage: www.elsevier.com/locate/stapro

A turning bands method for simulating isotropic Gaussian random fields on the sphere

Xavier Emery [a,b], Reinhard Furrer [c,*], Emilio Porcu [d]

[a] Department of Mining Engineering, University of Chile, Santiago, Chile
[b] Advanced Mining Technology Center, University of Chile, Santiago, Chile
[c] Department of Mathematics and Department of Computational Science, University of Zurich, 8057 Zurich, Switzerland
[d] School of Mathematics and Statistics, University of Newcastle, GB. Chair of Spatial Analytics Methods. & Department of Mathematics, University of Atacama, Copiapó, Chile

ARTICLE INFO

Article history:
Available online 31 July 2018

Keywords:
Covariance functions
Great circle
Spheres
Turning bands

ABSTRACT

We introduce a novel approach to simulate Gaussian random fields defined over spheres of $\mathbb{R}^3$. Through continuation we embed the process on the sphere in a nonstationary random field of $\mathbb{R}^3$ to use a turning bands method. We also discuss the approximation accuracy.

1. Introduction

The interest in modeling stochastic processes over spheres with an explicit covariance function is reflected in work in areas as diverse as mathematical analysis, probability theory, spatial point processes, geostatistics and mathematical physics, and the reader is referred to, e.g., Marinucci and Peccati (2011), Porcu et al. (2018) and Jeong et al. (2017) for comprehensive surveys.

There is a wealth of simulation algorithms for Gaussian random fields on d-dimensional Euclidean spaces. In particular, sequential Gaussian, Cholesky decomposition of the covariance matrix, Gibbs sampling, autoregressive and moving average, circulant embedding and discrete spectral methods have been designed to simulate Gaussian vectors that represent the random field at a finite set of points located in $\mathbb{R}^3$ (Chilès and Delfiner, 2012 with the references therein). A few other algorithms are also available to continuously simulate the random field over any domain of $\mathbb{R}^3$, among which the most widespread are the continuous spectral and turning bands methods (Shinozuka, 1971; Shinozuka and Jan, 1972; Matheron, 1973).

However, the natural metric on the sphere is the great circle distance, which describes an arc between any pair of points located over the spherical shell. Covariance functions depending on the great circle distance are called geodesically isotropic in Porcu et al. (2018). There is a lack of simulation methods for random fields over spheres whose covariance functions depend on the great circle distance, with the work of Lang and Schwab (2015), Creasey and Lang (2018), Le Gia et al. (2018), Fan et al. (2018) and Doroshkevich et al. (2005) being notable exceptions. The latter three references use the publicly available software HEALPix (http://healpix.sourceforge.net/) and GLESP scheme (http://www.glesp.nbi.dk/) to simulate isotropic Gaussian fields on the sphere.

Here, we present an alternative approach based on turning bands, which allows to construct realizations of random fields on spheres with covariance functions depending on the great circle distance. Additionally, the method allows for a reasonable trade-off between computational efficiency and accuracy of the realization.

* Corresponding author.
E-mail addresses: xemery@ing.uchile.cl (X. Emery), reinhard.furrer@math.uzh.ch (R. Furrer), emilio.porcu@newcastle.ac.edu (E. Porcu).

https://doi.org/10.1016/j.spl.2018.07.017

In the case of random fields defined over the Euclidean space $\mathbb{R}^3$, continuous spectral and turning bands methods are successful in this respect (Lantuéjoul, 2002; Emery and Lantuéjoul, 2006; Hunger et al., 2015; Emery et al., 2016). This paper considers the problem of generalizing these methods for Gaussian fields defined over the spherical shell of $\mathbb{R}^3$ and having a geodesically isotropic covariance function. In particular, our modeling strategy is the following:

- Given a Gaussian process on the unit sphere of $\mathbb{R}^3$, we consider its continuation to $\mathbb{R}^3$ in a way that the original random field and the new random field defined by continuation coincide on the sphere of $\mathbb{R}^3$;
- The second order properties of the Gaussian field obtained by continuation are then inherited from those of the original Gaussian field on the sphere. In particular, we show how to obtain its nonstationary spectral density;
- The turning bands method is extended to nonstationary processes of $\mathbb{R}^3$;
- Then, the desired simulations are obtained by restricting the nonstationary turning bands method to the sphere.

To our knowledge, our proposal represents the first attempt to adapt turning bands methods on the sphere.

The outline of the paper is the following. Section 2 describes isotropic Gaussian field on spheres and then provides the way to build the continuation of a Gaussian process on the sphere to a process on $\mathbb{R}^3$. Section 3 provides the turning bands algorithm. We also provide the second order moments and distribution of the simulated realizations. Practical implementation, together with some examples, are then proposed. We close the paper with a short discussion.

2. Random fields on spheres and their continuations to $\mathbb{R}^3$

2.1. Isotropic Gaussian processes on the sphere

We consider the sphere $\mathbb{S}^2$ of $\mathbb{R}^3$ with unit radius, *i.e.*, $\mathbb{S}^2 = \{\boldsymbol{s} \in \mathbb{R}^3 \,:\, \|\boldsymbol{s}\| = 1\}$, where $\|\cdot\|$ is the Euclidean norm. Every point $\boldsymbol{s}$ on the sphere has coordinates $\boldsymbol{s} = (\sin\vartheta\cos\varphi, \cos\vartheta\cos\varphi, \cos\vartheta)$, for $\vartheta \in [0, \pi]$ and $\varphi \in [0, 2\pi)$ being the latitude and azimuthal angles, respectively. We consider a real-valued random field Z on $\mathbb{S}^2$ and assume that the variance of $Z(\boldsymbol{s})$ is equal to 1 for any $\boldsymbol{s}$ on the sphere and that the covariance between $Z(\boldsymbol{s})$ and $Z(\boldsymbol{s}')$ depends exclusively on the great circle distance $\theta : \mathbb{S}^2 \times \mathbb{S}^2 \to [0, \pi]$, uniquely defined through

$$\theta = \theta(\boldsymbol{s}, \boldsymbol{s}') = \arccos\left(\langle \boldsymbol{s}, \boldsymbol{s}'\rangle\right), \qquad \boldsymbol{s}, \boldsymbol{s}' \in \mathbb{S}^2,$$

where $\langle\cdot,\cdot\rangle$ is the classical inner product. Under such an assumption, Schoenberg (1942)'s theorem shows that the covariance function C associated with Z admits the following expansion:

$$C(\theta) = \sum_{n=0}^{\infty} a_n P_n(\cos\theta), \qquad \theta \in [0, \pi], \tag{2.1}$$

where P_n denotes the nth Legendre polynomial, and where $\{a_n\}_{n=0}^{\infty}$ is a uniquely determined probability mass sequence, also called sequence of *Schoenberg coefficients* in Daley and Porcu (2013). Thus $C(0) = 1$ and hence C is a correlation function. Albeit we work always under this case and we use C for correlation or covariance equivalently, whenever no confusion can arise. Arguments in Dai and Xu (2013) and Marinucci and Peccati (2011) show that

$$Z(\boldsymbol{s}) = \sum_{n=0}^{\infty} \sum_{\ell=-n}^{+n} \mathcal{A}_{\ell,n} \mathcal{Y}_{\ell,n}(\boldsymbol{s}), \qquad \boldsymbol{s} \in \mathbb{S}^2, \tag{2.2}$$

where the set of spherical harmonics $\{\mathcal{Y}_{\ell,n}\}$ is an orthonormal basis for the space $\mathcal{L}_2(\mathbb{S}^2, \nu_2)$, with ν_2 being the Lebesgue measure on $\mathbb{S}^2$. Further, $\{\mathcal{A}_{\ell,n}\}_{\ell,n}$ is a bi-sequence of complex-valued random variables with zero mean and

$$\operatorname{cov}\left(\mathcal{A}_{\ell,n}, \mathcal{A}_{\ell',n'}\right) = \mathbb{E}\left(\mathcal{A}_{\ell,n}, \overline{\mathcal{A}_{\ell',n'}}\right) - \mathbb{E}\left(\mathcal{A}_{\ell,n}\right)\mathbb{E}\left(\overline{\mathcal{A}_{\ell',n'}}\right) = \frac{4\pi}{2n+1} a_n \delta_{\ell=\ell'} \delta_{n=n'},$$

with $\mathbb{E}$ denoting mathematical expectation, $\overline{\cdot}$ denoting complex conjugation, δ denoting the Kronecker delta and a_n as defined through Eq. (2.1). Using the addition theorem for spherical harmonics (Dai and Xu, 2013), we have that the process

$$Z^{(n)}(\boldsymbol{s}) := \sum_{\ell=-n}^{+n} \mathcal{A}_{\ell,n} \mathcal{Y}_{\ell,n}(\boldsymbol{s}), \qquad \boldsymbol{s} \in \mathbb{S}^2, \tag{2.3}$$

has covariance function $C^{(n)}(\theta) = a_n P_n(\cos\theta)$. This fact is essential for the construction we have in mind. In fact, if simulation of $Z^{(n)}$ becomes feasible at least until a given $n = n_o$, then the process Z can be simulated by truncating the expansion in Eq. (2.2) at n_o. Thus, we have that

$$Z_{\text{sim}}(\boldsymbol{s}) = \sum_{n=0}^{n_o} Z_{\text{sim}}^{(n)}(\boldsymbol{s}), \qquad \boldsymbol{s} \in \mathbb{S}^2, \tag{2.4}$$

becomes our target for the simulation.

2.2. Continuation of $Z^{(n)}$ to the whole space $\mathbb{R}^3$

For $n = 0, 1, \ldots$, let us define a random field $Y^{(n)}$ on $\mathbb{R}^3$ through the following identity:

$$Y^{(n)}(\boldsymbol{s}) = \begin{cases} r^N \exp(-\lambda(r^2-1)) Z^{(n)}\left(\dfrac{\boldsymbol{s}}{r}\right), & \boldsymbol{s} \in \mathbb{R}^3 \setminus \{0\}, \\ 0, & \boldsymbol{s} = 0, \end{cases}$$

where $\lambda > 0$, $N > 0$, $r = \|\boldsymbol{s}\|$, and with $Z^{(n)}$ as being defined by Eq. (2.3) with $a_n = 1$ for the sake of simplicity. Thus, $Y^{(n)}$ and $Z^{(n)}$ coincide on $\mathbb{S}^2$. Direct inspection shows that the covariance $C_Y^{(n)}$ associated with $Y^{(n)}$ admits expression

$$C_Y^{(n)}(\boldsymbol{s}, \boldsymbol{s}') = \exp(2\lambda)(r \times r')^N \exp\left(-\lambda(r^2 + r'^2)\right) C^{(n)}(\theta), \qquad \theta \in [0, \pi], \quad r, r' > 0. \tag{2.5}$$

Some comments are in order. First, the covariance function $C_Y^{(n)}$ is not stationary. Arguments in Yaglom (1961) show that $C_Y^{(n)}$ is the (generalized) Fourier transform of some nonnegative and bounded measure, F_n. Namely,

$$C_Y^{(n)}(\boldsymbol{s}, \boldsymbol{s}') = \int_{\mathbb{R}^3} \int_{\mathbb{R}^3} \exp\left(\imath\langle \boldsymbol{s}, \boldsymbol{\omega}\rangle - \imath\langle \boldsymbol{s}', \boldsymbol{\omega}'\rangle\right) F_n(\mathrm{d}(\boldsymbol{\omega}, \boldsymbol{\omega}')), \qquad \boldsymbol{s}, \boldsymbol{s}' \in \mathbb{R}^3, \tag{2.6}$$

where $\imath$ is the complex number such that $\imath^2 = -1$. Throughout, we suppose F_n to be absolutely continuous with respect to the Lebesgue measure, so that $F_n(\mathrm{d}(\boldsymbol{\omega}, \boldsymbol{\omega}')) = f_n(\boldsymbol{\omega}, \boldsymbol{\omega}')\mathrm{d}\boldsymbol{\omega}\mathrm{d}\boldsymbol{\omega}'$. Additionally, we can observe that $C_Y^{(n)}$ is symmetric, so that Eq. (2.6) simplifies into

$$C_Y^{(n)}(\boldsymbol{s}, \boldsymbol{s}') = \int_{\mathbb{R}^3} \int_{\mathbb{R}^3} \cos\left(\langle \boldsymbol{s}, \boldsymbol{\omega}\rangle - \langle \boldsymbol{s}', \boldsymbol{\omega}'\rangle\right) f_n(\boldsymbol{\omega}, \boldsymbol{\omega}')\mathrm{d}\boldsymbol{\omega}\mathrm{d}\boldsymbol{\omega}', \qquad \boldsymbol{s}, \boldsymbol{s}' \in \mathbb{R}^3. \tag{2.7}$$

Arguments in Yadrenko (1983) show that $Y^{(n)}(\boldsymbol{s}) = \int \exp(\imath\langle \boldsymbol{s}, \boldsymbol{\omega}\rangle) W^{(n)}(\mathrm{d}\boldsymbol{\omega})$, where $W^{(n)}$ is a complex random measure such that $\mathbb{E}\left(W^{(n)}(\mathrm{d}\boldsymbol{\omega})\overline{W^{(n)}}(\mathrm{d}\boldsymbol{\omega}')\right) = f_n(\boldsymbol{\omega}, \boldsymbol{\omega}')\mathrm{d}\boldsymbol{\omega}\mathrm{d}\boldsymbol{\omega}'$. This fact proves that f_n is a positive semi-definite function.

By Fourier inversion, we get

$$f_n(\boldsymbol{\omega}, \boldsymbol{\omega}') = \frac{1}{(2\pi)^6} \int_{\mathbb{R}^3} \int_{\mathbb{R}^3} \cos\left(\langle \boldsymbol{\omega}, \boldsymbol{s}\rangle - \langle \boldsymbol{\omega}', \boldsymbol{s}'\rangle\right) C_Y^{(n)}(\boldsymbol{s}, \boldsymbol{s}')\mathrm{d}\boldsymbol{s}\mathrm{d}\boldsymbol{s}', \qquad \boldsymbol{\omega}, \boldsymbol{\omega}' \in \mathbb{R}^3, \tag{2.8}$$

which shows that f_n is real-valued and symmetric, insofar as C_Y is real-valued and symmetric.

To illustrate our findings, we introduce the ${}_1F_1$ hypergeometric function through the series representation

$${}_1F_1(a; b; z) = \sum_{k=0}^{\infty} \frac{(a)_k}{(b)_k} \frac{z^k}{k!}, \qquad z > 0,$$

where $a, b > 0$ and where $(a)_k$ denotes the kth Pochhammer symbol of a. Let $\omega = \|\boldsymbol{\omega}\|$ and $\omega' = \|\boldsymbol{\omega}'\|$. Also, let α be the angle between $\boldsymbol{\omega}$ and $\boldsymbol{\omega}'$. We have all the ingredients to propose the following result.

Theorem 2.1. *Let $n \in \mathbb{N}$, $N > 0$ and $\lambda > 0$. Let $f_n : \mathbb{R}^3 \times \mathbb{R}^3 \to \mathbb{R}$ be the function defined by Eq. (2.8). Then,*

$$f_n(\boldsymbol{\omega}, \boldsymbol{\omega}') = \exp(2\lambda) P_n(\cos\alpha) \frac{\Gamma^2\left(\frac{n+N+3}{2}\right)(\omega\omega')^n}{(2\pi)^3 2^{2n+3} \lambda^{n+N+3} \Gamma^2\left(n + \frac{3}{2}\right)} {}_1F_1\left(\frac{n+N+3}{2}; n + \frac{3}{2}; -\frac{\omega^2}{4\lambda}\right)$$
$$\times\ {}_1F_1\left(\frac{n+N+3}{2}; n + \frac{3}{2}; -\frac{\omega'^2}{4\lambda}\right), \qquad \boldsymbol{\omega}, \boldsymbol{\omega}' \in \mathbb{R}^3. \tag{2.9}$$

The proof of this theorem is deferred to the Supplementary Material.

3. Simulation algorithm

Let K be a (large) positive integer. In what follows, we consider a probability density function $g : \mathbb{R}^d \to \mathbb{R}_+$ such that the support of $g \otimes g$ includes that of f_n, where $\otimes$ denotes the tensor product between two functions. We then consider the following ingredients:

1. A sequence $\{\boldsymbol{\omega}_k\}_{k=1}^K \overset{\text{iid}}{\sim} g$;
2. Let $\Omega = (\boldsymbol{\omega}_1, \ldots, \boldsymbol{\omega}_K)^\top$, with $\top$ denoting the transpose of a vector. We define the matrix $S_n(\Omega)$, having dimension $K \times K$, whose generic element $S_{k,k'}^{(n)}$ is defined by

$$S_{k,k'}^{(n)} = \frac{2 f_n(\boldsymbol{\omega}_k, \boldsymbol{\omega}_{k'})}{g(\boldsymbol{\omega}_k) g(\boldsymbol{\omega}_{k'})}, \qquad k, k' \in 1, \ldots, K.$$

The matrix $S_n(\Omega)$ inherits the properties of the function f_n in Eq. (2.8). Thus, $S_n(\Omega)$ is positive semi definite, which implies that there exists a matrix $A_n(\Omega)$ such that $S_n(\Omega) = A_n(\Omega)A_n^T(\Omega)$. For instance, $A_n(\Omega)$ could be the principal square root of $S_n(\Omega)$;

3. A Gaussian random vector $\boldsymbol{U} = (U_1, \ldots, U_K)^\top$, with mutually independent elements U_k, $k \in 1, \ldots, K$ and such that $\mathbb{E}U_k = 0$ and $\mathbb{E}U_k^2 = 1$ for all k;
4. A vector $\boldsymbol{B}_n(\Omega) = (B_1^{(n)}, \ldots, B_K^{(n)})^\top$ defined through

$$\boldsymbol{B}_n(\Omega) = A_n(\Omega)\boldsymbol{U};$$

5. A random variable ϕ uniformly distributed over the interval $[0, 2\pi]$. Additionally, ϕ, $\boldsymbol{U}$ and Ω are mutually independent.

We now define

$$Y_{\text{sim}}^{(n)}(\boldsymbol{s}) = \frac{1}{K}\sum_{k=1}^{K} B_k^{(n)} \cos\left(\langle \boldsymbol{\omega}_k, \boldsymbol{s}\rangle + \phi\right), \qquad \boldsymbol{s} \in \mathbb{R}^d. \tag{3.1}$$

Before proceeding, we note that as f_n is real-valued, then so will be the components of $\boldsymbol{B}_n(\Omega)$, and thus $Y_{\text{sim}}^{(n)}$ will be real-valued as well.

3.1. Moments and distribution of $Y_{\text{sim}}^{(n)}$

We now provide the first and second order moments of $Y_{\text{sim}}^{(n)}$. As for the mean, the fact that ϕ, $\boldsymbol{U}$ and Ω are mutually independent implies that $\mathbb{E}Y_{\text{sim}}^{(n)}(\boldsymbol{s}) = 0$ for all $\boldsymbol{s} \in \mathbb{R}^d$. As for the covariance, direct inspection gives

$$\begin{aligned}
\widetilde{C}_Y^{(n)}(\boldsymbol{s}, \boldsymbol{s}') &:= \operatorname{cov}\left(Y_{\text{sim}}^{(n)}(\boldsymbol{s}), Y_{\text{sim}}^{(n)}(\boldsymbol{s}')\right) \\
&= \frac{1}{K^2}\sum_{k}^{K}\sum_{k'}^{K} \mathbb{E}_{\Omega,\phi,\boldsymbol{U}}\left(B_k^{(n)}B_{k'}^{(n)} \cos(\langle \boldsymbol{\omega}_k, \boldsymbol{s}\rangle + \phi)\cos(\langle \boldsymbol{\omega}_{k'}, \boldsymbol{s}'\rangle + \phi)\right) \\
&= \frac{1}{K^2}\sum_{k}^{K}\sum_{k'}^{K} \mathbb{E}_{\Omega,\phi}\left(\mathbb{E}_{\boldsymbol{U}}\left(B_k^{(n)}B_{k'}^{(n)}|\Omega, \phi\right)\cos(\langle \boldsymbol{\omega}_k, \boldsymbol{s}\rangle + \phi)\cos(\langle \boldsymbol{\omega}_{k'}, \boldsymbol{s}'\rangle + \phi)\right).
\end{aligned} \tag{3.2}$$

Using the trigonometric identity

$$\cos(\langle \boldsymbol{\omega}_k, \boldsymbol{s}\rangle + \phi)\cos(\langle \boldsymbol{\omega}_{k'}, \boldsymbol{s}'\rangle + \phi) = \frac{1}{2}\cos(\langle \boldsymbol{\omega}_k, \boldsymbol{s}\rangle + \langle \boldsymbol{\omega}_{k'}, \boldsymbol{s}'\rangle + 2\phi) + \frac{1}{2}\cos(\langle \boldsymbol{\omega}_k, \boldsymbol{s}\rangle - \langle \boldsymbol{\omega}_{k'}, \boldsymbol{s}'\rangle).$$

and the fact that ϕ is uniform over $[0, 2\pi]$, we have that $\widetilde{C}_Y^{(n)}$ in (3.2) simplifies into

$$\widetilde{C}_Y^{(n)}(\boldsymbol{s}, \boldsymbol{s}') = \frac{1}{2K^2}\sum_{k}^{K}\sum_{k'}^{K} \mathbb{E}_{\Omega}\left(S_{kk'}^{(n)}\ \cos(\langle \boldsymbol{\omega}_k, \boldsymbol{s}\rangle - \langle \boldsymbol{\omega}_{k'}, \boldsymbol{s}'\rangle)\right) =: \frac{1}{2K^2}\sum_{k}^{K}\sum_{k'}^{K} \mathbb{E}_{\Omega}\alpha_{kk'}^{(n)}. \tag{3.3}$$

Since our main goal is to simulate a realization of a random field Z with covariance function C as defined in Eq. (2.1), it becomes important to evaluate the discrepancy between $\widetilde{C}_Y^{(n)}$ and $C_Y^{(n)}$. We now have two cases for the terms of Eq. (3.3):

- $k \neq k'$ ($K(K-1)$ terms are involved). Through direct inspection we obtain

$$\begin{aligned}
\mathbb{E}\alpha_{kk'}^{(n)} &= \mathbb{E}\left(S_{kk'}^{(n)}\ \cos(\langle \boldsymbol{\omega}_k, \boldsymbol{s}\rangle - \langle \boldsymbol{\omega}_{k'}, \boldsymbol{s}'\rangle)\right) \\
&= \int_{\mathbb{R}^3}\int_{\mathbb{R}^3} \frac{2f_n(\boldsymbol{\omega}_k, \boldsymbol{\omega}_{k'})}{g(\boldsymbol{\omega}_k)g(\boldsymbol{\omega}_{k'})}\cos(\langle \boldsymbol{\omega}_k, \boldsymbol{s}\rangle - \langle \boldsymbol{\omega}_{k'}, \boldsymbol{s}'\rangle)g(\boldsymbol{\omega}_k)g(\boldsymbol{\omega}_{k'})\mathrm{d}\boldsymbol{\omega}_k\mathrm{d}\boldsymbol{\omega}_{k'} \\
&= 2C_Y^{(n)}(\boldsymbol{s}, \boldsymbol{s}');
\end{aligned}$$

- $k = k'$ (K terms involved). We get

$$\mathbb{E}\alpha_{kk}^{(n)} = \int_{\mathbb{R}^3} \frac{2f_n(\boldsymbol{\omega}_k, \boldsymbol{\omega}_k)}{g^2(\boldsymbol{\omega}_k)}\cos(\langle \boldsymbol{\omega}_k, \boldsymbol{s} - \boldsymbol{s}'\rangle)g(\boldsymbol{\omega}_k)\mathrm{d}\boldsymbol{\omega}_k. \tag{3.4}$$

The last expression shows that there might be a discrepancy between $\widetilde{C}_Y^{(n)}$ and $C_Y^{(n)}$. However, if the ratio $2f_n(\boldsymbol{\omega}_k, \boldsymbol{\omega}_k)/g^2(\boldsymbol{\omega}_k)$ is bounded, and for K large, we get that $\widetilde{C}_Y^{(n)}$ is a good approximation of $C_Y^{(n)}$. At the same time, this implies some restriction – in our case guidance – on the choice of g.

As for the distribution of $Y_{\text{sim}}^{(n)}$, in order to get a random field whose finite-dimensional distribution are approximately multivariate Gaussian, we can resort to the central limit theorem and define

$$Y_{\text{final}}^{(n)}(\boldsymbol{s}) = \frac{1}{\sqrt{L}} \sum_{l=1}^{L} Y_{\text{sim}}^{(n,l)}(\boldsymbol{s}), \qquad \boldsymbol{s} \in \mathbb{R}^d, \tag{3.5}$$

where L is a (large) positive integer, and where $Y_{\text{sim}}^{(n,l)}$, $l = 1, \ldots, L$ are independent copies of $Y_{\text{sim}}^{(n)}$. The study of the convergence of $Y_{\text{final}}^{(n)}$ to a Gaussian random field as L becomes infinitely large is out of the scope of this paper and deserves further research.

3.2. Practical implementation

We now consider the function f_n as defined in Eq. (2.9). Direct computation shows that $f_n(\boldsymbol{\omega}, \boldsymbol{\omega}) \to 0$ when $\omega \to 0$. Also, we have that $f_n(\boldsymbol{\omega}, \boldsymbol{\omega}) \sim \omega^{-2N-6}$ when $\omega \to \infty$. This aspect, in concert with an appropriate choice of λ and N, is of vital importance when choosing a density g such that the ratio $f_n(\boldsymbol{\omega}, \boldsymbol{\omega})/g^2(\boldsymbol{\omega})$ is bounded. Consider the following implementation:

1. Choose $N = n$, so that, for all $a > 0$, ${}_1F_1(a; a; z) = \exp(z)$, $z > 0$. The spectral density f_n in Eq. (2.9) becomes
$$f_n(\boldsymbol{\omega}, \boldsymbol{\omega}') = \frac{\exp(2\lambda)}{(2\pi)^3(2\lambda)^{2n+3}} P_n(\cos\alpha)(\omega\omega')^n \exp\bigl(-(\omega^2 + \omega'^2)/(4\lambda)\bigr), \qquad \boldsymbol{\omega}, \boldsymbol{\omega}' \in \mathbb{R}^3,$$
where all the other variables have been defined in Theorem 2.1.
2. Choose g such that the product $g(\boldsymbol{\omega})g(\boldsymbol{\omega}')$ is the closest possible to $f_n(\boldsymbol{\omega}, \boldsymbol{\omega}')$. An obvious choice is
$$g(\boldsymbol{\omega}) = \widetilde{g}(\omega; \kappa, n, \lambda) = \kappa\omega^n \exp(-\omega^2/(4\lambda)), \tag{3.6}$$
which means that the orientation of $\boldsymbol{\omega}$ is uniform (g is radially symmetric). To find out the normalization constant κ, let us integrate g on $\mathbb{R}^3$:
$$1 = \int_{\mathbb{R}^3} g(\boldsymbol{\omega})\mathrm{d}\boldsymbol{\omega} = 4\pi\kappa \int_{\mathbb{R}_+} \omega^{n+2} \exp(-\omega^2/(4\lambda))\mathrm{d}\omega. \tag{3.7}$$
The integrand in (3.7) is, up to a normalization factor, the probability density function of a chi variable with $n + 3$ degrees of freedom. Summing up, we have that g in (3.6) admits expression
$$g(\boldsymbol{\omega}) = \frac{1}{16\pi 2^n \lambda^{(n+3)/2} \Gamma((n+3)/2)} \omega^n \exp(-\omega^2/(4\lambda)).$$
3. We can now evaluate the ratio
$$\frac{2f_n(\boldsymbol{\omega}, \boldsymbol{\omega}')}{g(\boldsymbol{\omega})g(\boldsymbol{\omega}')} = \frac{8\exp(2\lambda)}{\pi\lambda^n} \Gamma^2((n+3)/2) P_n(\cos\alpha).$$
4. Accordingly, the square root of the matrix $S_n(\Omega)$ with generic entry $2f_n(\boldsymbol{\omega}, \boldsymbol{\omega}')/g(\boldsymbol{\omega})/g(\boldsymbol{\omega}')$ is
$$A_n(\Omega) = \exp(\lambda)\sqrt{\frac{8}{\pi\lambda^n}}\, \Gamma((n+3)/2) \widetilde{A}_n(\Omega),$$
$\widetilde{A}_n(\Omega)$ is the principal square root of the matrix with generic entry $P_n(\cos\alpha)$.
5. We thus have that $2f_n(\boldsymbol{\omega}, \boldsymbol{\omega})/g^2(\boldsymbol{\omega})$ does not depend on $\boldsymbol{\omega}$ and is identically equal to $\exp(2\lambda)/(\pi\lambda^n)\Gamma^2((n+3)/2)$, which is minimal when $\lambda = n/2$. This choice of λ therefore minimizes the approximation made in our algorithm. That means that it minimizes the bias in the covariance of the simulated field, originating from the K diagonal terms of the matrix $S_n(\Omega)$ with generic entry $2f_n(\boldsymbol{\omega}, \boldsymbol{\omega}')/g(\boldsymbol{\omega})/g(\boldsymbol{\omega}')$.

As an illustration, Fig. 1 depicts realizations of (3.5) obtained with $K = 1500$, $L = 100$, for $n = 2, 4, 6, 8$ from top left to bottom right. These realizations look like random perturbations of the spherical harmonics of degrees 2, 4, 6 and 8, respectively.

4. Discussion

While a formal assessment of the different approximations of the simulation method is beyond the scope of the paper, we close with a discussion about the bias associated with (3.4) as well as the other errors and the computational complexity of the proposed algorithm.

Direct inspection shows that Eq. (3.4) can be rewritten as

$$\mathbb{E}\alpha_{kk}^{(n)} = \frac{8\mathrm{e}^{2\lambda}\Gamma^2\left(\frac{n+3}{2}\right)}{\pi\lambda^n} \int_{\mathbb{R}^3} \cos\left(\langle\boldsymbol{\omega}, \boldsymbol{s} - \boldsymbol{s}'\rangle\right) g(\boldsymbol{\omega})\mathrm{d}\boldsymbol{\omega}.$$

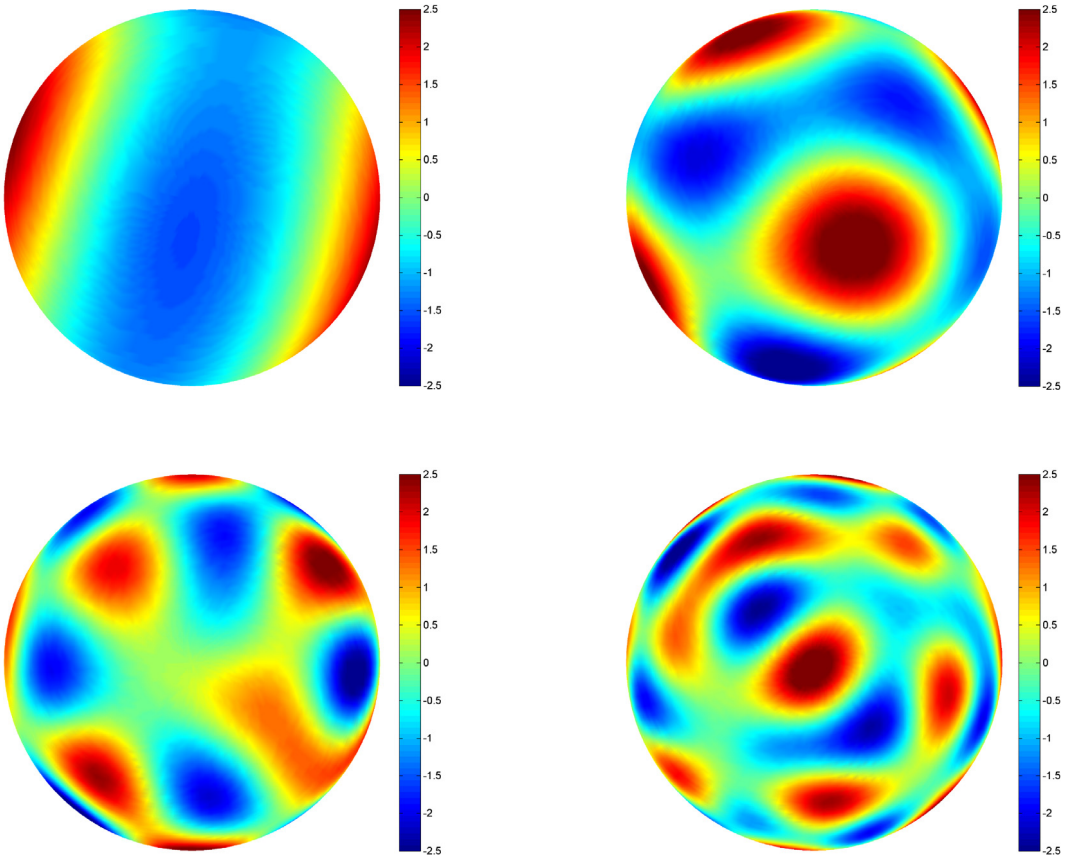

Fig. 1. From top left to bottom right: realizations of (3.5) for $K = 1500$, $L = 100$, and for $n = 2, 4, 6, 8$.

Using the fact that g is radially symmetric to convert the triple integral (a three-dimensional Fourier transform) into a single integral (a Hankel transform of order 3), in concert with equation 6.631.1 in Gradshteyn and Ryzhik (2007), we obtain that the above identity simplifies into

$$\mathbb{E}\alpha_{kk}^{(n)} = \frac{8\mathrm{e}^{2\lambda}\Gamma^2\left(\frac{n+3}{2}\right)}{\pi\lambda^n}\ {}_1F_1\left(\frac{n+3}{2};\frac{3}{2};-\lambda\|\boldsymbol{s}-\boldsymbol{s}'\|^2\right).$$

In particular, for $\boldsymbol{s} = \boldsymbol{s}'$ this expression reduces to

$$\mathbb{E}\left(\alpha_{kk}^{(n)}\right)_{\boldsymbol{s}=\boldsymbol{s}'} = \frac{8\mathrm{e}^{2\lambda}\Gamma^2\left(\frac{n+3}{2}\right)}{\pi\lambda^n},$$

and such a quantity is minimal when $\lambda = n/2$, in which case, by direct computation in concert with Stirling's formula, we get that

$$\mathbb{E}\left(\alpha_{kk}^{(n)}\right)_{\boldsymbol{s}=\boldsymbol{s}'} \sim 4(n+1)^2,$$

which vanishes for $(n+1)^2 \ll K$.

The error induced by truncating the expansion at n_o and using the process (2.4) can be directly controlled by coefficients a_n. Finally, error due to Eq. (3.5) has no impact on the discrepancy between $\widetilde{C}_Y^{(n)}$ and $C_Y^{(n)}$.

From a computational viewpoint, the advantages of the proposed algorithm are twofold. On the one hand, the memory storage requirements are minimal (of order $O(K^2)$ for the matrices $S_n(\Omega)$ and $A_n(\Omega)$), insofar as the simulated values can be written out as soon as they are generated and do not need to be kept in memory, which allows the simulation at any desired resolution on the sphere. On the other hand, the algorithm has essentially operation count $O(M \cdot L \cdot n_o \cdot K \cdot K^3)$, where M is the number of points on the sphere we simulate for, L is the number of summands linked to invoke the central limit theorem (see (3.5)), n_o the truncation order (see (2.4)) and K as illustrated in (3.1). For each realization, we need the $K \times K$ matrix $A_n(\Omega)$, accounting for K^3 in the operation count.

Acknowledgments

XE and EP acknowledge the support of grant CONICYT/FONDECYT/REGULAR/No. 1170290 from the Chilean Commission for Scientific and Technological Research, Chile. RF acknowledges the support of the Swiss National Science Foundation, Switzerland SNSF-175529.

Appendix A. Supplementary data

Supplementary material related to this article can be found online at https://doi.org/10.1016/j.spl.2018.07.017.

References

Chilès, J., Delfiner, P., 2012. Geostatistics: Modeling Spatial Uncertainty. Wiley, New York.
Creasey, P.E., Lang, A., 2018. Fast generation of isotropic gaussian random fields on the sphere. Monte Carlo Methods Appl. 24, 1–11.
Dai, F., Xu, Y., 2013. Approximation Theory and Harmonic Analysis on Spheres and Balls. Springer.
Daley, D.J., Porcu, E., 2013. Dimension walks and Schoenberg Spectral Measures. Proc. Amer. Math. Soc. 141, 1813–1824.
Doroshkevich, A.G., Naselsky, P.D., Verkhodanov, O.V., Novikov, D.I., Turchaninov, V.I., Novikov, I.D., Christensen, P.R., Chiang, L.Y., 2005. Gauss–Legendre sky pixelization (GLESP) for CMB maps. Internat. J. Modern Phys. D 14 (02), 275–290.
Emery, X., Arroyo, D., Porcu, E., 2016. An improved spectral turning-bands algorithm for simulating stationary vector Gaussian random fields. Stoch. Environ. Res. Risk Assess. 30 (7), 1863–1873.
Emery, X., Lantuéjoul, C., 2006. TBSIM: A computer program for conditional simulation of three-dimensional gaussian random fields via the turning bands method. Comput. Geosci. 32 (10), 1615–1628.
Fan, M., Paul, D., Lee, T.C.M., Matsuo, T., 2018. A multi-resolution model for non-Gaussian random fields on a sphere with application to ionospheric electrostatic potentials. Ann. Appl. Stat. 12 (1), 459–489.
Gradshteyn, I.S., Ryzhik, I.M., 2007. Tables of Integrals, Series, and Products, seventh ed.. Academic Press, Amsterdam.
Hunger, L., Cosenza, B., Kimeswenger, S., Fahringer, T., 2015. Spectral turning bands for efficient gaussian random fields generation on GPUs and accelerators. Concurr. Comput.: Pract. Exper. 27 (16), 4122–4136.
Jeong, J., Jun, M., Genton, M., 2017. Covariance models for global spatial statistics. Statist. Sci. 32, 501–513.
Lang, A., Schwab, C., 2015. Isotropic gaussian random fields on the sphere: regularity, fast simulation and stochastic partial differential equations. Ann. Appl. Probab. 25, 3047–3094.
Lantuéjoul, C., 2002. Geostatistical Simulation: Models and Algorithms. Springer, Berlin.
Le Gia, Q., Sloan, I., Womersley, R., Wang, Y., 2018. Sparse isotropic regularization for spherical harmonic representations of random fields on the sphere. Arxiv, arXiv:1801.03212.
Marinucci, D., Peccati, G., 2011. Random fields on the Sphere, Representation, Limit Theorems and Cosmological Applications. Cambridge, New York.
Matheron, G., 1973. The intrinsic random functions and their applications. Adv. Appl. Probab. 5 (2), 439–468.
Porcu, E., Alegría, A., Furrer, R., 2018. Modeling temporally evolving and spatially globally dependent data. Internat. Statist. Rev. First published: 24 May 2018, http://dx.doi.org/10.1111/insr.12266.
Schoenberg, I.J., 1942. Positive definite functions on spheres. Duke Math. J. 9, 96–108.
Shinozuka, M., 1971. Simulation of multivariate and multidimensional random processes. J. Acoust. Soc. Am. 49 (1B), 357–367.
Shinozuka, M., Jan, C., 1972. Digital simulation of random processes and its applications. J. Sound Vib. 25 (1), 111–128.
Yadrenko, A.M., 1983. Spectral Theory of Random Fields. Optimization Software, New York.
Yaglom, A.M., 1961. Second-order homogeneous Random Fields. In: Proc. 4th Berkeley Symp. Math. Stat. Prob. Vol. 2, pp. 593–622.